

A Numerical Evaluation of Electric Field and SAR Distribution Around a Titanium Implant in the Trunk of a Child

Abstract. The paper presents a numerical evaluation of electric field and SAR distribution in the trunk of a 6-year-old boy. The analysis was done for two cases – a boy's trunk with and without an implant. The electric field and SAR distribution were compared with regard to reference levels recommended by EU. The summary of results indicates that a conductive object in between tissues does not cause notable local enhancement both in the electric field and SAR distribution.

Streszczenie. W artykule przedstawiono numeryczną analizę rozkładu pola elektrycznego i współczynnika SAR w tułowiu sześciolatniego chłopca. Analizę wykonano dla dwóch przypadków: model tułowia z implantem i bez niego. Uzyskane rozkłady pola elektrycznego i SARu odniesione zostały do norm rekomendowanych przez UE. Zaprezentowana analiza wykazała, że obecność implantu nie powoduje znaczących zmian w rozkładzie pola elektrycznego i SARu. (Numeryczna analiza rozkładu pola elektrycznego i SAR w tułowiu dziecka z tytanowym implantem).

Słowa kluczowe: metalowy implant, pole elektryczne, SAR, normy ochronne.

Keywords: metallic implant, electric field, SAR, safety standards.

Introduction

The environment is constantly exposed to electromagnetic field (EMF). The influence of EMF on living organisms is of various ways and results in different effects. One of its effects is the therapeutic one [1]. However, it should be consciously controlled by indicating, for example, safety zones [2]. It results from the fact that the reaction of organism on EMF depends on many factors, such as the quantity of absorbed energy, time of exposure, and EMF frequency. The frequency dependence divides the EMF effects into two main parts: physiological effects caused by eddy currents (low frequency) and thermal effects caused by dielectric losses (high frequency). The latter ones are demonstrated by SAR coefficient (Specific Absorption Rate).

In order to evaluate SAR distribution in a human body a lot of factors have to be taken under the consideration. The most important ones are shown in Fig. 1. One should notice that the absorbed EMF energy depends on the proper identification of the frequency of the field as well as the physical and geometrical parameters of the object, i.e. the human tissue dielectric parameters and the metallic implant.

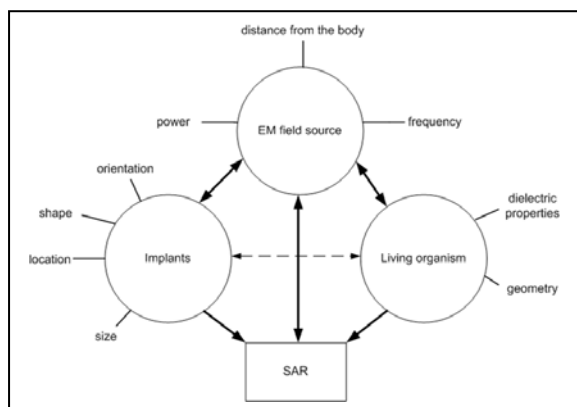


Fig. 1. The factors which determine SAR distribution in human body

It should be also underlined that the evaluation of SAR distribution is a very sophisticated task due to the fact that all the factors influence one another.

There are many adults who carry metallic implants inside their bodies. In general, these implants can be

divided into two groups i.e. passive implants like orthopedic plates, wires, rods and active ones like, for example, pacemakers. Moreover, children can carry metallic items such as titanium bars in the case of, for example, pectus excavatum deformity which produces sunken appearance of the chest [3] (see Fig. 2).



Fig. 2. X-Ray of a 15-year-old male after undergoing the Nuss procedure [3]

One of the methods of pectus excavatum treatment is called Nuss procedure [3], which involves slipping in one or more concave steel bars into the chest, underneath the sternum. The bar is flipped to a convex position so as to push outward on the sternum, correcting the deformity. The bar usually stays in the body for about two years, although many surgeons are now moving towards leaving them in for up to five years. When the bones have solidified into place, the bar is removed through outpatient surgery.

Whenever a RF field impinges on such a metallic object, the field is scattered around the conductor and may redistribute the energy of the incident field to produce peak SAR concentrations around the parts of the implant. SAR is the fundamental metric of RF heating and can be calculated in any point of the exposure material from the internal electric field (E) using:

$$(1) \quad SAR = \frac{\sigma}{\rho} |E|^2 = c \frac{\Delta T}{\Delta t}$$

where σ is the conductivity (S/m), ρ is the mass density (kg/m^3), and E is expressed in rms (V/m). It should be underlined that the relation (1) to temperature is limited to an „ideal” case with no heat loss by thermal diffusion, heat radiation or thermoregulation.

The standards which contemporary exist do not identify the case of human body with an implant. It may evoke the problems as the permitted values of SAR and current density in the body can be exceeded and this fact may bring unclear and ambiguous interpretation. Therefore, the norms should take into account the occurrence of the implants in the human body. Such work is already being conducted by some groups [4]-[6]. At this place, it seems to be justified to quote the EU recommendation, based on ICNIRP's [7] data which give all the EMF limitations. One should notice that the limitations are divided into two parts: 1) basic restrictions which give the values of electromagnetic quantities occurring in the human body (see Tables 1 and 2) the reference values, which manifest the electromagnetic values, and which the human body is exposed to (Table 2).

Table 1. Basic restriction on current density and SAR based on ICNIRP

Frequency	Current density (mA/m ²) (rms)	Whole body average SAR (W/kg)	Localized SAR (head and trunk) (W/kg)	S (W/m ²)
1 -100 kHz	f/500	-	-	-
0.1 -10 MHz	f/500	0,08	2	-
10 MHz-10 GHz	-	0,08	2	-
10-300 GHz	-	-	-	10

Table 2. Levels for electric, magnetic and electromagnetic fields (800 Hz to 300 GHz, unperturbed rms values)

Frequency range	E-field strength (V/m)	H-field strength (A/m)	B-field (μT)	S (W/m ²)
0,8- 3 kHz	250/f	5	6,25	-
3-150 kHz	87	5	6,25	-
0,15-1 MHz	87	0,73/f	0,92/f	-
1-10 MHz	87/ f ^{1/2}	0,73/f	0,92/f	-
10-400 MHz	28	0,073	0,092	2
400-2000 MHz	1,375 f ^{1/2}	0,0037 ^{1/2}	0,0046 f ^{1/2}	f/200
2-300 GHz	61	0,16	0,20	10

Numerical model

The induced SAR in a human body can be calculated using the FDTD method. In this study we have explored the method of numerical modelling for assessing a metallic implant influence on SAR and electric field distribution in the realistic three-dimensional geometry, based on Virtual Family [8] (see Fig. 3.)



Fig. 3. Virtual Family (from left to right: Ella, Duke, Billie, Thelonious)

In our case we have used Thelonious, 6-year-old male child model. In order to hasten the calculations and save a work station operating memory we have used the trunk instead of the whole model. In Fig. 4 the model with an implanted titanium bar is shown.

The dielectric properties (electrical conductivity σ relative permittivity ϵ_r) and mass density (ρ) used in this study were specified by [9] and calculated for the frequency 2.45 GHz. The following dielectric properties were assigned to the

titanium bar: $\sigma = 5.9$ (S/m), $\epsilon_r = 1$, $\rho = 4700$ (kg/m³). A uniform plane-wave incident on the front of the body was used as the excitation throughout this study (see Fig. 3). The electric field (E) was parallel to the long axis of the body. This polarization was chosen as the worst one i.e. the one which induces the highest whole-body SAR as it was shown previously in [10]. Such a field would simulate a human in the far-field of a radiating source like, for example, a base station antenna.

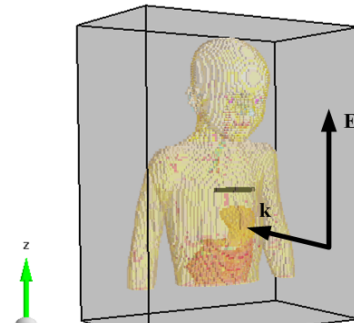


Fig. 4. The model used in the calculations, i.e. Thelonious's trunk with titanium bar. The black arrows indicate the plane wave polarization.

Analysis and results

In order to investigate the implanted titanium bar influence on the electric field and SAR distribution two scenarios were considered: the trunk with an implant and without it. The model was exposed to a constant uniform ambient power flux density of 10 W/m². The power flux value was chosen in accordance with ICNIRP reference levels (see Table 2 for frequency range 2-300 GHz).

The electric field results for the boy trunk are presented in Fig. 5-left and Fig. 6-left prior to the titanium bar being implanted into it, whereas in Fig. 5-right and Fig. 6-right they are presented together with the titanium bar.

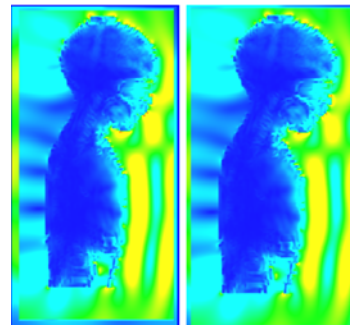


Fig. 5. Electric field distribution at 2.45 GHz in the boy trunk (without the bar - left; with the bar - right); sagittal plane

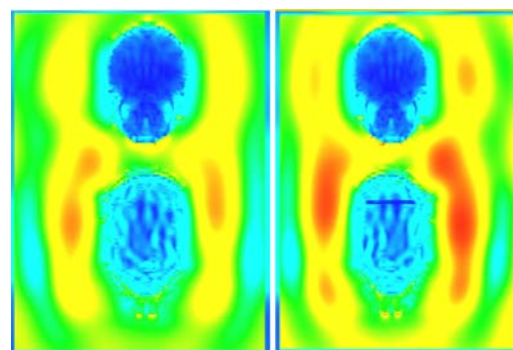


Fig. 6. Electric field distribution at 2.45 GHz in the boy trunk (without the bar - left; with the bar - right); coronal plane

The only noticeable differences in the electric field distributions between the models with the titanium bar and without it occur in vicinity of shoulders and neck. In the case with the bar there are higher electric field spots outside the chest, but around the implanted bar there is almost no difference in the electric field distribution.

The analogous distributions to the above electric field can be seen in Fig. 7-left and 7-right where SAR averaged to 10 grams of a tissue is presented.

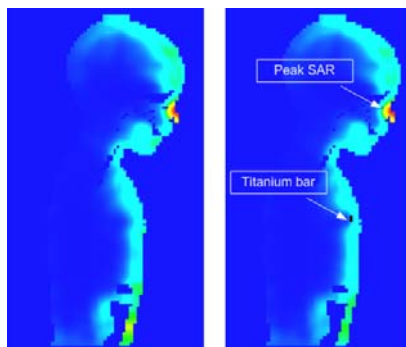


Fig. 7. SAR distribution at 2.45 GHz in the boy trunk (without the bar - left; with the bar - right); sagittal plane

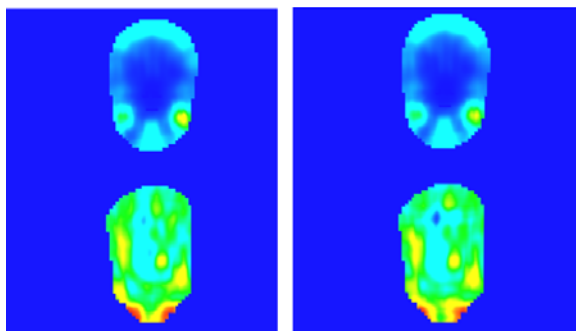


Fig. 8. SAR distribution at 2.45 GHz in the boy's trunk (without the bar - left; with the bar - right); coronal plane

As for SAR distributions, the differences between the trunk with the titanium bar compared to the trunk without the bar occur near the bar, where SAR goes deeper into the chest as it can be seen in Fig. 7-right when compared with SAR distribution shown in Fig. 7-left. One should notice that the spots seen in Fig. 8-left did not change the position when the titanium bar was presented as shown in Fig. 8-right. Moreover, when comparing max values of SAR the cooling impact of the titanium bar can be seen as shown in Table 3. The peak SAR in both models occurred near the nose.

Table 3. Comparison of maximum values of electric field and SAR for the cases with and without the titanium bar

In vicinity of the implant	Without implant	With implant
Max E-field [V/m]	24.12	21.36
SAR _{10g} [W/kg]	0.426	0.408

Conclusions

In this study, it has been shown how EMF interacts with a metallic passive implant. A case study of titanium bar implanted into boy's trunk was presented. Electric field and SAR distributions have been calculated using FDTD method with regard to EU norm. The boy trunk model was exposed to a plane wave from the front with an electric field vector parallel to the long axis of the body, when an incident power flux density was 10 W/m². On the base of the calculations one can conclude that due to the interaction of the implant and RF field, the location of the highest SAR spots did not shift to the proximity of the implant. Moreover, on the base of maximum SAR's values the implant cooling effect can be observed.

REFERENCES

- [1] Gas P., Temperature Distribution of Human Tissue in Interstitial Microwave Hyperthermia, *Electrical Review*, 88 (2012), No. 7a, 144-146.
- [2] Cieřła A., et al., Determination of safety zones in the context of the magnetic field impact on the surrounding during magnetic therapy, 87 (2011), *Electrical Review (Przegląd Elektrotechniczny)*, 79-82.
- [3] http://en.wikipedia.org/wiki/Pectus_excavatum
- [4] MacIntosh R.L., et al., A numerical Evaluation of SAR and Temperature Changes Around a Matallic Plate in the Head of a RF Exposed Worker, *Bioelectromagnetics*, (2005), vol. 26, 377-388
- [5] Virtanen H., Keshavari J., Lappalainen R., Interaction of Radio Frequency Electromagnetic Fields and Passive Metallic Implants - A Brief Review, (2006), vol. 27, 431-439
- [6] S. A. Mohsin, J. Nyenhuis, R. Masood, Interaction of Medical Implants with The MRI Electromagnetic Fields, *Progress In Electromagnetics Research C*, (2010), Vol. 13, 195-202.
- [7] International Commission on Non-Ionizing Radiation Protection (ICNIRP) 1998 Guidelines for Limiting Exposure to Time-varying Electric, Magnetic, and Electromagnetic Fields (up to 300 GHz), *Health Physics*, 74: 494-522
- [8] www.itis.ethz.ch/virtualpopulation
- [9] Hasgall P.A., Neufeld E., Gosselin M.C., Klingenböck A., Kuster N., IT'IS Database for thermal and electromagnetic parameters of biological tissues, Version 2.2, July 11th, 2012. www.itis.ethz.ch/database
- [10] Miaskowski A., Krawczyk A., The influence of the electromagnetic wave polarization on SAR in human body model, (2006) *Przegląd Elektrotechniczny*, 82 (5), pp. 61-62.

Autorzy: dr inż. Arkadiusz Miaskowski, University of Life Sciences in Lublin, Department of Applied Mathematics and Computer Science, Akademicka 13, 20-950 Lublin, Poland, E-mail: arek.miaskowski@up.lublin.pl; dr hab. Grażyna Olchowik, Medical University of Lublin, Department of Biophysics, Jaczewskiego 4, 20-090 Lublin, E-mail: grazyna.olchowik@umlub.pl; prof. Andrzej Krawczyk, Częstochowa University of Technology, Armii Krajowej 17, Częstochowa, Poland, E-mail: ankra.new@gmail.com; mgr inż. Ewa Łada-Tondyra, Częstochowa University of Technology, Armii Krajowej 17, Częstochowa, Poland, E-mail: ewalada@interia.eu; mgr inż. Andrzej Bartosiński, Military Institute of Hygiene and Epidemiology, 4 Kozielska St. 01-163 Warsaw, Poland, E-mail: albartosinski@gmail.com